 doi:10.20944/preprints202107.0195.v1

Article

Loop-mediated isothermal amplification in core-shell beads assay for the detection of tyrosine kinase AXL over expression

Kamalalayam Rajan Sreejith[a‡], Muhammad Umer [a‡], Pradip Singha[a], Nhat-Khuong Nguyen[a], Surasak Kasetsirikul[a,b], Chin Hong Ooi[a], Muhammad J. A. Shiddiky*[b] and Nam-Trung Nguyen*[a]

[a] Queensland Micro- and Nanotechnology Centre, Griffith University, 170 Kessels Road, 4111 Queensland, Australia;
[b] School of Environment and Science, Nathan Campus, Griffith University, 170 Kessels Road, 4111 Queensland, Australia;
‡ Both the authors contributed equally to the work
* Corresponding authors: nam-trung.nguyen@griffith.edu.au; m.shiddiky@griffith.edu.au

Abstract: The upregulated expression of thyrosine kinase AXL has been reported in several hematologic and solid human tumors including gastric, breast, colorectal, prostate, and ovarian cancers. Thus, AXL can potentially serve as a diagnostic and prognostic biomarker for various cancers. This paper reports the first-ever use of loop-mediated isothermal amplification (LAMP) of the AXL gene as a diagnostic method for ovarian cancer. We demonstrated simple instrumentation toward a point-of-care device to perform LAMP. This paper also reports the first-ever use of core-shell beads as a microreactor to perform LAMP as an attempt to promote environmentally friendly laboratory practices.

Keywords: Loop-mediated isothermal amplification; AXL over expression; core-shell beads assay.

1. Introduction

The receptor tyrosine kinase AXL initially identified to be overexpressed in human myeloid leukemia cells has over the years emerged as a promising diagnostic and therapeutic target for a range of cancers [1]. The AXL receptor is activated by binding of ligand growth arrest specific gene-6 (GAS6). Several major cellular signaling pathways like PI3K-AKT-mTOR, NF-kB, and JAK/STAT are activated downstream of the GAS6-AXL binding event indicating the pivoting role that AXL plays in normal cellular functioning [2]. AXL signaling is involved in cell proliferation and survival, cell adhesion and migration, and regulation of inflammatory cytokines. AXL is overexpressed in several cancers including gastric, breast, colorectal, prostate, and ovarian cancers. Overexpression of AXL is found to be involved in angiogenesis, resistance to chemotherapy, and attenuated antitumor immune response. AXL also plays an important role in epithelial to mesenchymal transformation (EMT), cell invasion, and migration, highlighting its role in cancer metastasis. As a result, AXL has been extensively explored not only as a therapeutic target but also as a diagnostic and prognostic marker [1,2].

Among molecular diagnostic tools, isothermal amplification methods have attracted widespread interest in recent years as possible alternatives to the gold standard polymerase chain reaction (PCR) based analyses [3,4] As these isothermal amplification reactions are carried out at a constant temperature, reliance on sophisticated thermal cyclers can be eliminated. Therefore, these isothermal amplification methods can prove to be an attractive approach for the development of point-of-care molecular analysis platforms. Among the various isothermal amplification methods, loop-mediated isothermal amplification (LAMP) is the most widely used technique [4]. LAMP offers several advantages such as high specificity due to the use of 4-6 primers, tolerance to inhibitors, and the ability to directly detect RNA without the requirement of reverse transcription step. Taken together, LAMP appears to be a suitable method of choice for point-of-care applications [5].

Preprints (www.preprints.org) | NOT PEER-REVIEWED | Posted: 8 July 2021 doi:10.20944/preprints202107.0195.v1

However, despite the simplicity of the procedure, detection of the amplified product is still a significant challenge. Although naked-eye colorimetric or turbidimetric methods for the detection of LAMP products have been widely used, these methods provide qualitative information at best. In situations where accurate quantification of the target may be required, such as monitoring the expression level of cancer related genes such as AXL, a more robust detection method may be needed. Fluorescent detection of LAMP amplicons may be more appropriate in this case; however, it requires sophisticated instrumentation.

All molecular diagnostic tools including LAMP are currently carried out in conventional plastic vials or conventional microfluidic chips. Approximately 5.5 million tons of plastic waste was reported to be generated only from biolabs around the world in 2014 [6]. Conventional molecular diagnostic methods such as PCR and LAMP add a significant contribution to this. The recent development of microfluidics and microtechnologies allows for the integration of flow control [7] and temperature control [8,9] on a chip, making the compact implementation of PCR and LAMP possible. However, conventional microfluidic chips are not a solution for the reduction of non-reusable plastic waste they generate. Droplet-based microfluidics has a great potential in reducing sample size and using temperature control not only for the reaction but also for droplet actuation [10]. This paper reports the use core-shell beads as a droplet-based microreactor to carry out LAMP reaction. Core shell beads belongs to the emerging field of micro elastofluidics [11], consisting of a core liquid embedded in a transparent hard spherical shell. Core-shell beads are one promising replacement to conventional plastic vials and microfluidic chips. Core-shell beads could reduce the amount of plastic waste by 86% [12]. Core-shell bead was also demonstrated to serve as a microreactor for PCR [12,13]. However, to the best of our knowledge, no study was reported to utilize core-shell beads as a microreactor for LAMP. Furthermore, no study has been reported on LAMP of AXL genes as a potential candidate for diagnosing certain cancers. The present paper reports the use of LAMP in core-shell beads to detect AXL overexpression as a potential diagnostic tool for cancer detection.

2. Materials and Methods

2.1 Cell Culture and Isolation of RNA

Immortalized human mesothelial cell line MeT-5A was purchased from American Type Culture Collection (ATCC), USA. Cells were cultured in T-25 cell culture flasks using RPMI 1640 medium supplemented with 10% heat-inactivated fetal bovine serum (FBS), 100 U/mL penicillin, and 100 mg/mL streptomycin. Cultures were maintained in a humidified incubator at 37 °C with 5% CO_2. Cells were harvested by trypsinization at 70-80% confluence and pelleted by centrifuging at 2000×g for 5 min. RNA was isolated from pelleted cells using Monarch total RNA miniprep kit (Cat # T2010S, NEB Australia) following manufacturer's protocol. Purified RNA was finally eluted in nuclease free water. The quality and quantity of the RNA was analyzed by NanoDrop spectrophotometer.

2.2 Preparation of LAMP reaction mixture

A 214 bp long synthetic target corresponding to the positions 1688-1901 of AXL transcript variant 2, mRNA reference sequence (NM_001699.6) was used as template to optimize the reaction conditions. Table 1 lists the template and primer sequences. Target sequence was isothermally amplified using WarmStart® LAMP Kit (DNA & RNA), (Cat # E1700S, NEB Australia) in a 10 µL reactor as per manufacturer's instructions. The reaction mix consisted of 5 µL of WarmStart LAMP 2X Master Mix, 0.2 µL of 50× fluorescent dye, and 1 µL of 10× primer mix (final concentrations: FIP/BIP 1.6 µM, F3/B3 0.2 µM). A volume of 1 µL of synthetic target of known copy number was used and the reaction was made up to 10 µL using nuclease free water (Cat # 10977015, ThermoFisher Australia). For cell

Preprints (www.preprints.org) | NOT PEER-REVIEWED | Posted: 8 July 2021 doi:10.20944/preprints202107.0195.v1

line LAMP, 100 ng of total RNA isolated from Met-5A cells was used as a template. Real

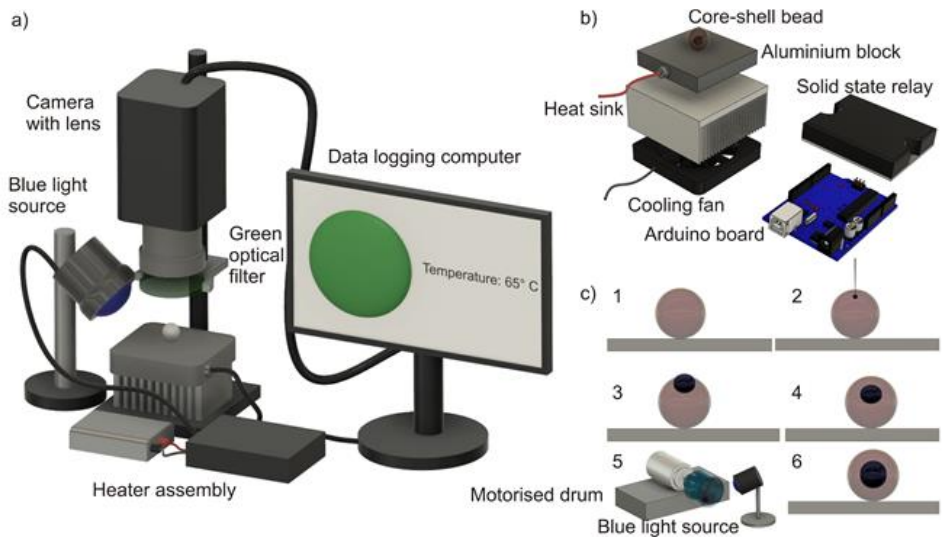

Fig 1. Core-shell bead-based LAMP: a) Experimental setup; b) Exploded view of the heater platform. c) Various stages of core-shell bead synthesis.

time monitoring of change in fluorescence levels during the LAMP reaction was carried out in parallel on CFX96 Touch Real-Time PCR Detection System (Bio-Rad), to compare the functionality and efficiency of LAMP in core-shell beads. Samples were incubated on 65°C for 45 minutes and fluorescence signal was recorded in FAM channel after every minute. The reaction was stopped by denaturing Bst 2.0 and RTx enzymes at 85°C for 5 minutes. The melt curve analysis of amplified products was carried out by heating for 5 seconds each between 65°C and 95°C at 0.5°C increments. Data collection was enabled at each increment of the temperature.

Table 1: LAMP template and primer sequences

Name	Sequence
AXL_F3	CCTGGGCATCAGTGAAGAG
AXL_B3	CGCTTCACTCAGGAAATCCT
AXL_FIP	TCCAAACTCTCCCTCTCCCAGATTTTGGGATGTGA TGGTGGACCG
AXL_BIP	ATGGAAGGCCAGCTCAACCAGTTTTCCTCGTGCAG ATGGCAATC
Synthetic target	CCTGGGCATCAGTGAAGAGCTGAAGGAGAAGCTG CGGGATGTGATGGTGGACCGGCACAAGGTGGCCC TGGGGAAGACTCTGGGAGAGGGAGAGTTTGGAGC TGTGATGGAAGGCCAGCTCAACCAGGACGACTCCA TCCTCAAGGTGGCTGTGAAGACGATGAAGATTGCC ATCTGCACGAGGTCAGAGCTGGAGGATTTCCTGAG TGAAGCG

2.3 Preparation of core-shell beads

The core-shell beads required for this experiment were made using liquid marble technology. Liquid marbles are liquid droplets coated with fine particles of hydrophobic

Preprints (www.preprints.org) | NOT PEER-REVIEWED | Posted: 8 July 2021 doi:10.20944/preprints202107.0195.v1

or oleophobic powder [14]. Liquid marbles find applications in cell biology, sensing, disease diagnosis and pathogen detection [15-17]. Liquid marbles also serve as a microreactor platform to carry out biochemical reactions [18-20]. However, the evaporation of liquid marbles at elevated temperature limits their use in reactions carried out at elevated temperatures [21-25]. The liquid marble technology can be used to synthesize core-shell beads with a hard shell. And a hard shell would prevent evaporation. In this experiment, we used a photopolymer as the shell liquid and the LAMP reaction mixture as the core liquid.

An amount of 0.05 g of camphorquinone and 0.06 g of ethyl-4-(dimethylamino) benzoate in 10 g of Trimethylolpropane trimethacrylate (TRIM) were mixed well in a glass beaker using a magnetic stirrer at 600 rpm for 2 minutes. The prepared photopolymer mixture was stored in an opaque container for future use. Trimethylolpropane trimethacrylate is a crosslinking monomer. To the best of our knowledge, no cytotoxicity was reported for TRIM, and this compound has been frequently used in dentistry and for making bone cement [26,27].

A super amphiphobic silicon monolith called "marshmallow-like gel" (MG) [28] was used as the oleophobic material for synthesizing core shell beads. MG was received from one of our collaborators in Kagoshima University, Japan. The delicate thin sheets of MG were powdered using mortar and collected in an open plastic plate (35 mm x 35 mm x 10 mm), forming a super amphiphobic powder bed.

Various steps involved in the synthesis of core-shell bead using liquid marble technology are depicted in Figure 1c. In step 1, 20 µl of previously prepared photopolymer liquid was deposited on to the amphiphobic powder bed. In step 2, 2 µl of LAMP mixture was injected into the photopolymer liquid droplet using a micropipette. In step 3, the LAMP mixture was observed to be partially immersed in the photopolymer, however exposing almost one third of its volume to the environment. Photopolymerization of the outer liquid at this stage will not be efficient as the sample liquid may evaporate during heating of the bead. In step 4, the composite liquid phase obtained from step 3 was gently rolled over the powder bed to get the droplet coated with the powder and to generate a composite liquid marble. A composite liquid marble is a liquid phase (core liquid) covered with another liquid phase (shell liquid), which is again covered with a solid phase (amphiphobic powder). We observed that the one third portion of the core liquid which was exposed to the ambient was just subsided beneath the exterior photopolymer liquid after coating it with the powder. This is due to the high "phobic" nature of the core liquid to the powder than the photopolymer liquid. A photopolymerization at this stage will result in a core shell bead. However, the thickness of the shell above the core liquid will be relatively thin and may be prone to breakage due to thermal stress during the heating process. It is better to position the core liquid to the center of photopolymer to avoid this problem. In step 5, the composite liquid marble obtained after step 4 was transferred to a motorized cylindrical drum. The motorized drum was rotated at 140 rpm for 5 minutes with a blue light source kept at 5 cm above it, continuously illuminating the rotating composite liquid marble. It was already reported that the rotary motion of composite liquid marble would push the core liquid drop to the center of the exterior liquid.[29] In step 6, the process of simultaneous rotation and photopolymerization resulted in core-shell beads whose core liquid is relatively perfectly at the center of the hardened shell. The core shell bead obtained would be covered with amphibhobic powder. This can be cleaned by washing them in deionized water, resulting in transparent core-shell beads.

2.4 Design and fabrication of isothermal heater and fluorescent monitoring system

A commercial thermal cycler and fluorescent monitoring system for core-shell bead based LAMP is not available. Hence, we developed a customized thermal cycler and fluorescent monitoring system. An aluminum block (A 20 mm x 20 mm x 15 mm) embedded with a cartridge heater (5 mm diameter and 15-mm length, Core electronics) was used as the heating platform. The power to the heater was controlled using PID (proportional-integral-derivative) algorithm implemented in an Arduino UNO microcontroller board. The real time temperature of the heater block was monitored by an LM 35 temperature

Preprints (www.preprints.org) | NOT PEER-REVIEWED | Posted: 8 July 2021 doi:10.20944/preprints202107.0195.v1

sensor glued to the aluminum block and fed back to the Arduino board. The temperature setpoint was 67°C (+2K offset is provided to compensate for the temperature difference between the heater platform and the core-shell bead). The entire heater assembly was attached to an aluminum heat sink (85.6 mm × 68.3 mm × 41.5 mm) and a cooling fan assembly (12 V, 3,300 rpm, 70 mm × 70 mm × 25 mm). The heat sink and cooling fan assembly is implemented for safety purposes. The cooling fan will be activated and the power supply to the heater block will be disconnected if the temperature of the heater block exceeds 90°C, thus protecting the device from thermal runaway.

The excitation and emission spectra of the LAMP mixture were 450-490 nm (blue) and 520-560 nm (green) respectively. A customized excitation light source was formed by 30 circularly arranged blue LEDs. The excitation light source was powered by a 12 V, 3 A DC adapter. A vertically mounted CMOS camera (Edmund Optic EO-5012C) attached with a 0.5× telecentric lens (Edmund Optics-63074) and a green optical filter (520-560 nm) was used as the fluorescent detection device. The excitation source was automatically switched on in intervals of 10 minutes and the images of the fluorescence emission were captured simultaneously. The intermittent fluorescent excitation (with an interval of 10 minutes) was chosen to avoid photobleaching of the sample. Figure 1a depicts the experimental setup. Figure 1b shows the exploded view of the thermal cycler assembly. The custom-built thermal cycler demonstrated a ramping rate of 0.68 K/s during heating and a steady-state error of ±0.5K.

An additional dummy experiment was carried out to check whether the core-shell bead possesses the same temperature as the heater platform. 50 µL of photopolymer liquid was dropped onto the oleophobic powder bed and a thermistor (NTC 10) was inserted into the liquid photopolymer liquid drop. The droplet embedded with the thermistor was subsequently illuminated with blue light for 5 minutes. The photopolymerization of the liquid droplet provided a hardened bead embedded with the thermistor. This bead is subsequently placed on the heater platform. The platform was heated to 65°C, and the temperatures of the heater platform and of the bead were noted. There was an average temperature difference of 2.12K between the heater platform and the bead. Figure 2a shows the image of the bead embedded with the thermistor. Figure 2b depicts the thermal characteristics of the heater platform and the bead.

2.5 Experimental procedure

The first phase of the experiment was completed using synthetic DNA template corresponding to AXL mRNA RefSeq. Three different starting template copy numbers (C. Ns), 1×10^3, 1×10^5, and 1×10^7 were tested. A no template control (NTC) reaction was also included. The reactions were carried out on a real-time PCR machine.

The second phase of the experiments was completed using core-shell bead as a micro reactor and in a specially developed thermal cycler. Core-shell beads were prepared using 20 µL of photopolymer liquid and 2 µL of sample mixture as described in section 2.3. Core-shell beads containing three different starting template copy numbers 1×10^3, 1×10^5, and 1×10^7 were prepared. The core-shell beads were placed onto the isothermal heater below the telecentric lens of the fluorescent monitoring system, Fig. 1a. The isothermal

Preprints (www.preprints.org) | NOT PEER-REVIEWED | Posted: 8 July 2021 doi:10.20944/preprints202107.0195.v1

heater was preheated to 67°C instead of 65°C to compensate for the temperature differ-

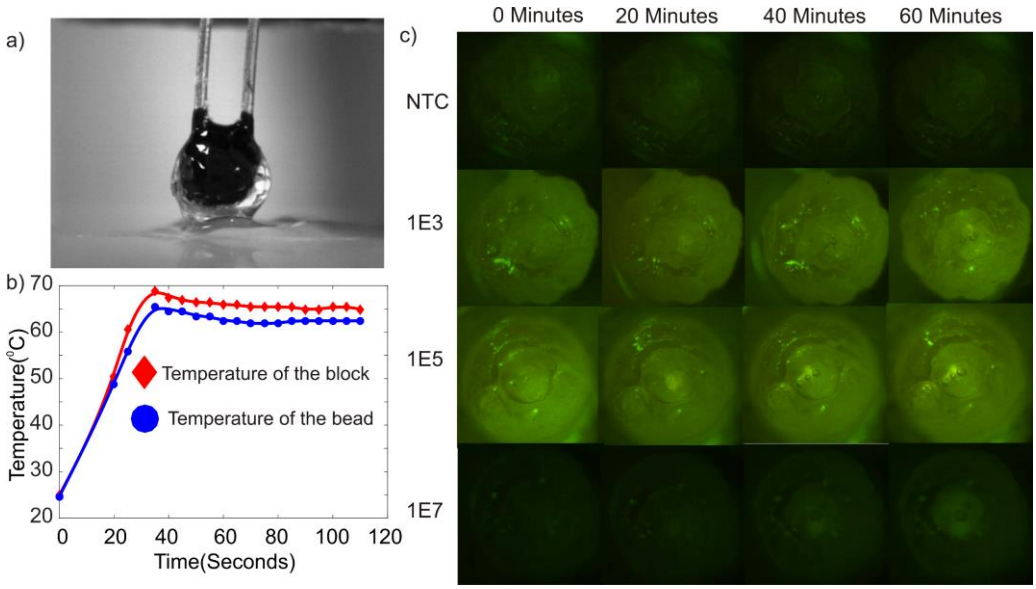

Fig 2. a Photograph of bead embedded with thermistor b) Temperature reading of the bead and the heater block c) Photographs of the core-shell beads at various times during the LAMP reaction

ence between the heater platform and the bead as noted in the dummy experiment. Samples containing NTC was subjected to LAMP for 60 minutes to observe, whether any amplification occured. Observing a negative amplification from samples containing NTC after 60 minutes, we decided to carry out the reactions in core-shell beads for 60 minutes instead of 45 minutes. This would provide a window for the reaction to be successful for a sample volume of 2 µL in a core-shell bead compared to a sample volume of 10 µL in a conventional machine. Experiments were repeated 3 times for each starting template concentration and for core-shell beads containing NTC.

We carried out LAMP reactions using Met-5A total RNA under similar reaction conditions. Total RNA isolated from cells was diluted to a concentration of 100 ng/µL using nuclease free water. A volume of 1 µL of total RNA was used as template in the LAMP reaction. The secondary phase of the experiment was completed using a cell line sample.

2.6 Image processing and data analysis

Images of core-shell beads under heating were taken periodically every 10 minutes for 60 minutes. The average pixel density of the circular region containing the sample was obtained using Image J software. This average pixel density was considered as the numerical equivalent of the fluorescence emitted from the core -shell bead. This numerical equivalent of the fluorescence was subsequently offset corrected and normalized to minimize disparity among the results and to provide better comparative study. Offset correction and normalization were implemented according to the equation

$$I_{st}^{*} = (I_{st} - I_{s0})/I_{max} \quad (1)$$

Where, I_{st} is the numerical equivalent of the fluorescent intensity of the sample at any instant, I_{s0} is the numerical equivalent of the fluorescent intensity of the corresponding sample at the beginning of the LAMP reaction and I_{max} is the numerical equivalent of the maximum fluorescent intensity obtained among all the samples tested. The standard error of the readings was calculated as:

Preprints (www.preprints.org) | NOT PEER-REVIEWED | Posted: 8 July 2021 doi:10.20944/preprints202107.0195.v1

$$S.E = \sigma/\sqrt{n} \quad (2)$$

$$\sigma = \sqrt{\frac{\sum(I^*_{st} - I^*_{st\_mean})^2}{n-1}} \quad (3)$$

where, $I^*_{st\_mean}$ is the average of the numerical equivalent of fluorescent intensities of various samples with same template concentration at an instant.

3. Results and discussion

Figure 3a shows the amplification of LAMP reactions as fluorescent signals (relative fluorescence unit, RFU) obtained from each sample versus time in a conventional commercial thermal cycler. Out of the three tested concentrations of the synthetic target, the primers used in this study could amplify only templates with up to 1×10^5 starting copy number. No amplification was observed up to 40 minutes of incubation with a template with 1×10^3 copies as the starting material. Similarly, we observed no amplification for the NTC samples up to 40 minutes. Both 1×10^3 sample and NTC showed a little amplification around 43 minutes. However, considering the low starting template concentration and NTC showed similar amplification trend, the detection limit of our assay in a conventional thermal cycler was 1×10^5 template copy number.

Figure 3b depicts the amplification obtained from LAMP reaction carried out in core-shell beads. In contrast to the results obtained from LAMP reaction carried out in conventional machine, the sample containing 1×10^3 starting copies showed a fluorescence emission after 20 minutes. Subsequently, the fluorescence followed grew steadily till 50 minutes. A sudden surge of fluorescence was observed after 60 minutes. This behavior could be considered as positive fluorescence since the samples containing NTC did not shown any fluorescence after 60 minutes. Samples containing an initial copy number of 1×10^5 and 1×10^7 showed a steady increase in fluorescence from the beginning to the end of the reaction. The end fluorescent intensity of the samples followed a logical pattern of $1\times10^7 > 1\times10^5 > 1\times10^3$. It should be noted that the fluorescent intensity values of samples containing initial template copy numbers of 1×10^5 and 1×10^7 already reached more than 80% of their corresponding maximum values after 45 minutes, provided that only 2 µL of the sample was used compared to LAMP in a conventional plastic vial. However, it is clear that a direct comparison of results from plastic vial based conventional LAMP with core-shell bead LAMP is not possible due to the difference is fluorescence detection methods and algorithms, the trend seen in the outcomes of core-shell bead based LAMP can be considered as a promising indication of them to be considered as an alternative for conventional methods. Our assay could detect a concentration as low as $1x10^5$ of starting copies on a conventional thermocycler. However, the assay sensitivity increased to about 500 fold in core-shell beads considering the reactions for core-shell beads were prepared initially in 10 µL out of which only 2 µL were used. Thus, detection limit achieved on core-shell beads was about 200 starting template copies. Although LAMP assays capable of detecting DNA molecules down to single copy numbers have been reported, particular sets of primers may be susceptible to false positives at low template concentrations [30].

Preprints (www.preprints.org) | NOT PEER-REVIEWED | Posted: 8 July 2021 doi:10.20944/preprints202107.0195.v1

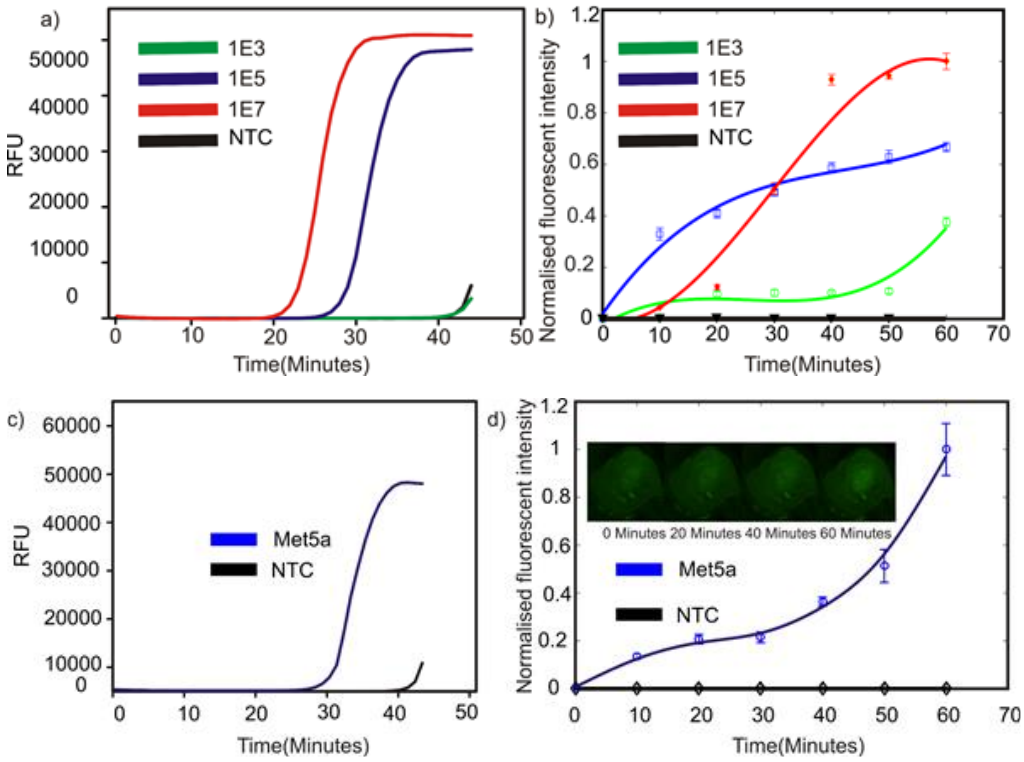

Fig 3. LAMP results: a) Synthetic target on a conventional qPCR platform. b) Synthetic target in cores-shell beads c) Met5a RNA on conventional qPCR platform d) Met5a RNA in core-shell beads.

Although determination of efficiency of LAMP assay is beyond the scope of this paper, further improvements in sensitivity of our platform are possible through careful optimization of LAMP primers, especially the inclusion of loop primers.

We further demonstrated the feasibility of LAMP assay for using total RNA isolated from Met-5A cell line. Met-5A is a human mesothelial cell line immortalized by the transformation of epithelial virus SV40. Met-5A expresses a high level of AXL RNA [31]. To the best of our knowledge, we described for the first time here a LAMP assay for detection of AXL in complex biological samples. AXL is an oncogene that is involved in several cancer promoting processes and is found to be overexpressed in a variety of cancers. AXL has emerged as a promising therapeutic target, and several AXL inhibitors are currently in clinical trials [1]. Therefore, the development of assays for AXL detection may be useful for pan-cancer diagnostics and theragnostics. We demonstrated that our platform can specifically detect AXL in a complex mixture of cellular RNA. RFU value for isothermal AXL amplification using Met-5A derived total RNA crossed the threshold at around 32 minutes on the conventional thermal cycler. However, using core-shell beads, a high fluorescent signal was observed as early as 10 minutes from the start of experiment. Amplification was observed for Met5a RNA at around 32 minutes. Effective heat transfer between the heater platform and the sample inside the core-shell bead and small sample volume in core-shell beads might be the possible factors leading to the improved amplification efficiency in core-shell beads. However, further research must be extended in this direction to gain more insight.

Although the core-shell bead-based LAMP assay demonstrated fluorescent output both at high and low template concentrations, the amplification curve of samples containing 1×10^7 template copies showed a lower fluorescence than those containing $1x10^5$ after 30 minutes. This discrepancy can be attributed to a few factors. First, the synthesis of core-shell bead was not optimized in terms of the quality of the core-shell bead. Due to this

 doi:10.20944/preprints202107.0195.v1

reason, the position of the core liquid can be different inside the shell in each bead. The geometric location of the core sample liquid plays an important role in the fluorescence emitted from the bead. Second, the transparency of the shell material could be another issue. Even though, the oleophobic powder is washed away from the bead after its synthesis, some residue of the powder may remain on the core-shell bead surface, affecting the fluorescence reading. Third, the lighting and fluorescence detection system were made from off-the-shelf components. Even a minute change in the illumination system can affect the fluorescence output. However, this discrepancy in the fluorescent intensity values at a time before the total reaction time of the LAMP is almost irrelevant as LAMP is vastly used for the end point detection.

4. Conclusions

Loop mediated isothermal amplification (LAMP) of 10-µL samples containing synthetic AXL genes were carried out in conventional plastic vials and thermal cycler. Successful amplification was recorded for samples containing 1×10^5 and 1×10^7 initial template copies. Samples containing 1×10^3 initial copies did not shown any amplification. Met5a cell line was also tested, yielding a positive amplification in conventional methods after 30 minutes. Subsequent experiments in core-shell beads using 2-µL sample volume in a specially developed thermal cycler yielded positive results. In contrast to the conventional method, samples containing 1×10^3 initial copy numbers demonstrated amplification in core-shell beads after 20 minutes and exhibited a peak fluorescence after 60 minutes. The samples containing copy number templates 1×10^5 and 1×10^7 also demonstrated amplification and the end point fluorescence followed a pattern $1\times10^7 > 1\times10^5 > 1\times10^3$. Subsequent experiment using Met5a cell line in core-shell bead demonstrated amplification after 10 minutes of heating. The fluorescent intensity was more than 10% of its maximum value after 10 minutes. It gave a fluorescent intensity of more than 30% of its maximum value after 40 minutes and the peak fluoresce was observed after 60 minutes of heating. Furthermore, we demonstrated the detection of AXL gene over expression using loop mediated isothermal amplification. We also demonstrated that the reaction can be carried out in a core-shell beads instead of a conventional plastic vials or a microfluidic device. The spherical shape of core-shell beads could provide a simple solution for focusing and detecting light [32] that potentially further simplify the design of the optical system. The simplicity of designing and developing a thermal cycler, as well as of the image detection hardware and simplicity of the image processing algorithm provides a larger window for engineering opportunities to develop an environmentally friendly point-of-care diagnostics for the detection of cancer using LAMP in core-shell beads.

Funding: The authors acknowledge the support of the Australian Research Council (DP180100055).

Acknowledgments: The work was performed in part in the Queensland node at Griffith of the Australian National Fabrication Facility, a company established under the National Collaborative Research Infrastructure Strategy to provide nano and microfabrication facilities for Australia's researchers. Authors also acknowledge Associate Prof. Takayuki Takei for generously donating the amphiphobic powder for the experiment.

Conflicts of Interest: There are no conflicts to declare.

References

1. Zhu, C.; Wei, Y.; Wei, X. AXL receptor tyrosine kinase as a promising anti-cancer approach: functions, molecular mechanisms and clinical applications. *Molecular Cancer* **2019**, *18*, 153, doi:10.1186/s12943-019-1090-3.
2. Gay, C.M.; Balaji, K.; Byers, L.A. Giving AXL the axe: targeting AXL in human malignancy. *British Journal of Cancer* **2017**, *116*, 415-423, doi:10.1038/bjc.2016.428.

3. Zhao, Y.; Chen, F.; Li, Q.; Wang, L.; Fan, C. Isothermal Amplification of Nucleic Acids. *Chemical Reviews* **2015**, *115*, 12491-12545, doi:10.1021/acs.chemrev.5b00428.
4. Tomita, N.; Mori, Y.; Kanda, H.; Notomi, T. Loop-mediated isothermal amplification (LAMP) of gene sequences and simple visual detection of products. *Nature Protocols* **2008**, *3*, 877-882, doi:10.1038/nprot.2008.57.
5. Ganguli, A.; Mostafa, A.; Berger, J.; Aydin, M.Y.; Sun, F.; Ramirez, S.A.S.d.; Valera, E.; Cunningham, B.T.; King, W.P.; Bashir, R. Rapid isothermal amplification and portable detection system for SARS-CoV-2. *Proceedings of the National Academy of Sciences* **2020**, *117*, 22727-22735, doi:10.1073/pnas.2014739117.
6. Urbina, M.A.; Watts, A.J.R.; Reardon, E.E. Labs should cut plastic waste too. *Nature* **2015**, *528*, 479, doi:10.1038/528479c.
7. Nguyen, N.T.; Schubert, S.; Richter, S.; Dötzel, W. Hybrid-assembled micro dosing system using silicon-based micropump/valve and mass flow sensor. *Sensors and Actuators A: Physical* **1998**, *69*, 85-91, doi:https://doi.org/10.1016/S0924-4247(98)00039-9.
8. Dinh, T.; Phan, H.; Qamar, A.; Woodfield, P.; Nguyen, N.; Dao, D.V. Thermoresistive Effect for Advanced Thermal Sensors: Fundamentals, Design Considerations, and Applications. *Journal of Microelectromechanical Systems* **2017**, *26*, 966-986, doi:10.1109/JMEMS.2017.2710354.
9. Dinh, T.; Phan, H.-P.; Dao, D.V.; Woodfield, P.; Qamar, A.; Nguyen, N.-T. Graphite on paper as material for sensitive thermoresistive sensors. *Journal of Materials Chemistry C* **2015**, *3*, 8776-8779, doi:10.1039/C5TC01650A.
10. Yap, Y.-F.; Tan, S.-H.; Nguyen, N.-T.; Murshed, S.M.S.; Wong, T.-N.; Yobas, L. Thermally mediated control of liquid microdroplets at a bifurcation. *Journal of Physics D: Applied Physics* **2009**, *42*, 065503, doi:10.1088/0022-3727/42/6/065503.
11. Nguyen, N.-T. Micro Elastofluidics: Elasticity and Flexibility for Efficient Microscale Liquid Handling. *Micromachines* **2020**, *11*, 1004.
12. Sreejith, K.R.; Gorgannezhad, L.; Jin, J.; Ooi, C.H.; Takei, T.; Hayase, G.; Stratton, H.; Lamb, K.; Shiddiky, M.; Dao, D.V., et al. Core-Shell Beads Made by Composite Liquid Marble Technology as A Versatile Microreactor for Polymerase Chain Reaction. *Micromachines* **2020**, *11*, 242.
13. Gorgannezhad, L.; Sreejith, K.R.; Christie, M.; Jin, J.; Ooi, C.H.; Katouli, M.; Stratton, H.; Nguyen, N.-T. Core-Shell Beads as Microreactors for Phylogrouping of E. coli Strains. *Micromachines* **2020**, *11*, 761.
14. Aussillous, P.; Quéré, D. Liquid marbles. *Nature* **2001**, *411*, 924-927, doi:10.1038/35082026.
15. Bormashenko, E. Liquid marbles: Properties and applications. *Current Opinion in Colloid & Interface Science* **2011**, *16*, 266-271, doi:10.1016/j.cocis.2010.12.002.
16. Nguyen, N.-K.; Ooi, C.H.; Singha, P.; Jin, J.; Sreejith, K.R.; Phan, H.-P.; Nguyen, N.-T. Liquid Marbles as Miniature Reactors for Chemical and Biological Applications. *Processes* **2020**, *8*, 793.
17. Vadivelu, R.; Kashaninejad, N.; Sreejith, K.R.; Bhattacharjee, R.; Cock, I.; Nguyen, N.-T. Cryoprotectant-Free Freezing of Cells Using Liquid Marbles Filled with Hydrogel. *ACS applied materials & interfaces* **2018**, *10*, 43439-43449, doi:10.1021/acsami.8b16236.
18. Sreejith, K.R.; Gorgannezhad, L.; Jin, J.; Ooi, C.H.; Stratton, H.; Dao, D.V.; Nguyen, N.-T. Liquid marbles as biochemical reactors for the polymerase chain reaction. *Lab on a Chip* **2019**, 10.1039/C9LC00676A, doi:10.1039/C9LC00676A.
19. Jin, J.; Ooi, C.H.; Sreejith, K.R.; Zhang, J.; Nguyen, A.V.; Evans, G.M.; Dao, D.V.; Nguyen, N.-T. Accurate dielectrophoretic positioning of a floating liquid marble with a two-electrode configuration. *Microfluidics and Nanofluidics* **2019**, *23*, 85, doi:10.1007/s10404-019-2255-5.
20. Jin, J.; Sreejith, K.R.; Ooi, C.H.; Dao, D.V.; Nguyen, N.-T. Critical Trapping Conditions for Floating Liquid Marbles. *Physical Review Applied* **2020**, *13*, 014002, doi:10.1103/PhysRevApplied.13.014002.
21. Sreejith, K.R.; Ooi, C.H.; Dao, D.V.; Nguyen, N.-T. Evaporation dynamics of liquid marbles at elevated temperatures. *RSC Advances* **2018**, *8*, 15436-15443, doi:10.1039/c8ra02265h.

22. Dandan, M.; Erbil, H.Y. Evaporation rate of graphite liquid marbles: comparison with water droplets. *Langmuir : the ACS journal of surfaces and colloids* **2009**, *25*, 8362-8367, doi:10.1021/la900729d.
23. Bhosale, P.S.; Panchagnula, M.V.; Stretz, H.A. Mechanically robust nanoparticle stabilized transparent liquid marbles. *Applied Physics Letters* **2008**, *93*, 034109, doi:10.1063/1.2959853.
24. Laborie, B.; Lachaussée, F.; Lorenceau, E.; Rouyer, F. How coatings with hydrophobic particles may change the drying of water droplets: incompressible surface versus porous media effects. *Soft Matter* **2013**, *9*, 4822, doi:10.1039/c3sm50164g.
25. Aberle, C.; Lewis, M.; Yu, G.; Lei, N.; Xu, J. Liquid marbles as thermally robust droplets: coating-assisted Leidenfrost-like effect. *Soft Matter* **2011**, *7*, 11314, doi:10.1039/c1sm06480k.
26. Ono, S.; Kadoma, Y.; Morita, S.; Takakuda, K. Development of New Bone Cement utilizing Low Toxicity Monomers. *Journal of Medical and Dental Sciences* **2008**, *55*, 189-196, doi:10.11480/jmds.550201.
27. Vining, K.H.; Scherba, J.C.; Bever, A.M.; Alexander, M.R.; Celiz, A.D.; Mooney, D.J. Synthetic Light-Curable Polymeric Materials Provide a Supportive Niche for Dental Pulp Stem Cells. *Advanced materials* **2018**, *30*, 1704486, doi:10.1002/adma.201704486.
28. Hayase, G.; Kanamori, K.; Hasegawa, G.; Maeno, A.; Kaji, H.; Nakanishi, K. A Superamphiphobic Macroporous Silicone Monolith with Marshmallow-like Flexibility. *Angewandte Chemie International Edition* **2013**, *52*, 10788-10791, doi:10.1002/anie.201304169.
29. Takei, T.; Yamasaki, Y.; Yuji, Y.; Sakoguchi, S.; Ohzuno, Y.; Hayase, G.; Yoshida, M. Millimeter-sized capsules prepared using liquid marbles: Encapsulation of ingredients with high efficiency and preparation of spherical core-shell capsules with highly uniform shell thickness using centrifugal force. *J Colloid Interface Sci* **2019**, *536*, 414-423, doi:10.1016/j.jcis.2018.10.058.
30. Hardinge, P.; Murray, J.A.H. Reduced False Positives and Improved Reporting of Loop-Mediated Isothermal Amplification using Quenched Fluorescent Primers. *Scientific Reports* **2019**, *9*, 7400, doi:10.1038/s41598-019-43817-z.
31. Baird, A.-M.; Easty, D.; Jarzabek, M.; Shiels, L.; Soltermann, A.; Klebe, S.; Raeppel, S.; MacDonagh, L.; Wu, C.; Griggs, K., et al. When RON MET TAM in Mesothelioma: All Druggable for One, and One Drug for All? *Frontiers in Endocrinology* **2019**, *10*, doi:10.3389/fendo.2019.00089.
32. Song, C.; Nguyen, N.-T.; Tan, S.-H.; Asundi, A.K. Modelling and optimization of micro optofluidic lenses. *Lab on a Chip* **2009**, *9*, 1178-1184, doi:10.1039/B819158A.